Geohazard Mechanics 1 (2023) 1–17

Contents lists available at ScienceDirect

Geohazard Mechanics

journal homepage: www.keaipublishing.com/en/journals/geohazard-mechanics

Disturbance response instability theory of rock bursts in coal mines and its application

Yishan Pan *, Aiwen Wang

Institute of Disaster Rock Mechanics, Liaoning University, Shenyang, 110036, PR China

ARTICLE INFO

Keywords:
Coal mine
Rock burst
Coal mass deformation system
Control variables
Disturbance variables
Response variables
Coal mass stress
Stability theory
Circular roadway

ABSTRACT

Aiming at the rock burst prevention in coal mines, this study argue that a rock burst is the instability of the coal mass deformation system with the infinite deformation response subjected to a small disturbance, and the concepts of control, disturbance and response variables of the coal mass deformation system are proposed. The analytical solution of rock bursts of circular roadways is derived, using a mechanical model of the coal mass deformation system of circular roadways, and the stress and energy conditions of the disturbance response instability of a rock burst are also presented. Based on the disturbance response instability theory, this study identifies the factors controlling the occurrence of rock bursts, involving the coal uniaxial compressive strength, coal bursting liability and roadway support stress. The relationship between the critical stress and the critical resistance zone of surrounding rock in roadways, the coal uniaxial compressive strength, roadway support stress, roadway geometric parameters and coal burst liability is revealed, and the critical stress index evaluation method of rock burst risk is proposed. Considering the disturbance and response variables of rockburst occurrence, a monitoring system of rock burst based on stress and energy monitoring is established. Considering managing the disturbance and control variables, regional and local prevention measures of rock burst are proposed from four aspects: destressing in coal mass, avoiding the mutual disturbance between multi-group mining or excavation, reducing the dynamic load disturbance and weakening of the physical properties of the coal mass. Based on the enhancement principle of the roadway support stress on the critical load of rockburst occurrence and the energy absorption effect of the support, an energy absorption and anti-bursting support technology for roadways are proposed. The disturbance response instability theory of rock bursts has formed a technical system from the aspects of mechanism, prediction and prevention to guide the engineering practice for rock burst mitigation.

1. Introduction

Rock burst is a typical dynamic disaster related to mining activities in coal mines, manifesting as the sudden release of elastic energy from rock mass. It destroys the underground space and causes equipment damage and casualties, in some cases leading ground subsidence or earthquake. With the increase of mining depth, the intensity of rock burst is greater, the scope of damage is wider, the occurrence is more sudden, the rock-burst combined with other disasters increase. It is estimated that, by 2030, coal would still account for 55% of China's energy consumption, and nearly 10% of raw coal would come from coal mines with rock burst. Therefore, the prevention and control of rock burst is of great significance for mining safety and sustainability in deep underground coal mining in China.

Extensive research work and practical engineering have been conducted to solve the problem of rock bursts in coal mines [1,2], great progress has been made from the perspectives of mechanism, prediction, and prevention of rock bursts. Based on energy conservation, Cook et al. [3] proposed a rock burst theory, that stated, if the energy released during the mining process exceeded the energy dissipation, rock burst could be triggered. Bieniawski et al. [4] developed special experimental techniques and equipment for polyaxial rock testing for studies of failure characteristics of fractured rock, given results of tests on both soft and hard rock, proposed that the negative slopes of the stress-strain curves for fractured hard rock are much steeper than those for fractured soft rock. It also follows that hard rock is much more prone to violent rupture than soft rock. Petukhov et al. [5] argued that the rock burst is caused by strain softening of the material, which was defined as the stress exceeded the strength. Li et al. [6] proposed a “triple criteria” theory by summarizing the strength, energy and bursting liability theories. Zhang et al. [7,8]

* Corresponding author.
E-mail address: panyishan@lnu.edu.cn (Y. Pan).

https://doi.org/10.1016/j.ghm.2022.12.002
Received 13 October 2022; Received in revised form 13 December 2022; Accepted 15 December 2022
Available online 19 December 2022

argued that coal mass was in unstable state after strain softening, rock burst may be triggered by a small disturbance. Pan Yishan et al. [9,10] analysed the stability of rock structures in coal mines using the theory of limit point instability. Qingxin [11] argued that the material properties, bearing forces and the structure of surrounding rock are three main factors inducing rock burst. Dou Linming et al. [12] thought that the superposition of dynamic load and static load is the main reason of inducing rock burst. Jiang Fuxing [13] conducted the mechanism, prediction and control of "rock burst induced by shock bump" kind dynamic accident in composite thickness coal seam. Pan Junfeng et al. [14] stated that the progress of a rock burst can be divided into three stages: start-up, energy transfer and appearance. Manouchehrian et al. [15,16] pointed out that weak planes in the vicinity of deep roadways is an essential geo-condition for the occurrence of rockburst. Quantitative evaluation analysis is of great significance to the prevention and control of rock burst, Scholars have put forward many methods of prediction and evaluation of rock burst, such as a semi-quantitative coal burst risk classification system [17–19]. To prevent the rock burst in deep coal mines, Petr Koniek et al. [20,21] introduced rock blasting technology for pressure relief. Li CC et al. [22,23] presented principles of rock support for rockburst controlling and introduced three rockburst support systems used in deep metallic mines. These achievements made outstanding contributions to the prevention and control of rock burst occurred in coal mine, however, the problem of safety prevention and control of coal mine rock burst has not yet been solved.

From a viewpoint of dynamic phenomena, rock burst occurred in coal seam is the very similar with the rock burst occurred in hard rock induced by mining activities, however, the engineering environments of them are different. Several works have been conducted to analyse the relationship and difference between them in detail [24,25], this paper focuses on the rock burst occurred in coal mines.

The above theories partly reveal the occurrence mechanism of rockburst from different perspective, unfortunately, they all have some shortcomings. In detail, there is a lack of mathematical and mechanical model and bursting initiation criteria of rockburst, and a technical system for monitoring and prevention of rockburst based on occurrence theory has not been established. Based on the disturbance response instability theory of rockburst, this paper focuses on the essential factors controlling the rockburst occurrence, including mining stress, geostress, bursting tendency of coal material, and unifies the process of rockburst prevention and control, involving the disaster risk evaluation, monitoring, prevention and control, and the bursting-resistance support design in rockburst roadways. Thus, the instability theory of rockburst disturbance response will establish a complete system in terms of rockburst mechanism, prediction and prevention.

2. The disturbance response instability theory of rock bursts

2.1. Coal mass deformation system and its stability

The equilibrium state of a system can be divided into stable equilibrium and unstable equilibrium. The stable equilibrium situation is shown in Fig. 1(a). In the system composed of small ball and concave surfaces, if the ball deviates from the equilibrium position due to disturbance, the ball will swing back and forth around the original equilibrium position and finally return to the original equilibrium position. The situation of unstable equilibrium is shown in Fig. 1(b), if the ball deviates from the equilibrium position due to disturbance, and cannot return to the original equilibrium position, which is called unstable equilibrium. In this case, the equilibrium system composed of small ball and structural plane cannot maintain its original equilibrium state after external disturbance, it will lose stability and the ball releases potential energy at its original equilibrium position. Fig. 1(c) shows the coal mass deformation system of roadway. When the stress of the coal body exceeds the peak strength after the roadway excavation, the plastic deformation zone with energy dissipation is formed, and the surrounding coal mass constitutes the elastic deformation zone with energy storage. When the coal mass deformation system reaches an unstable equilibrium state, the coal mass

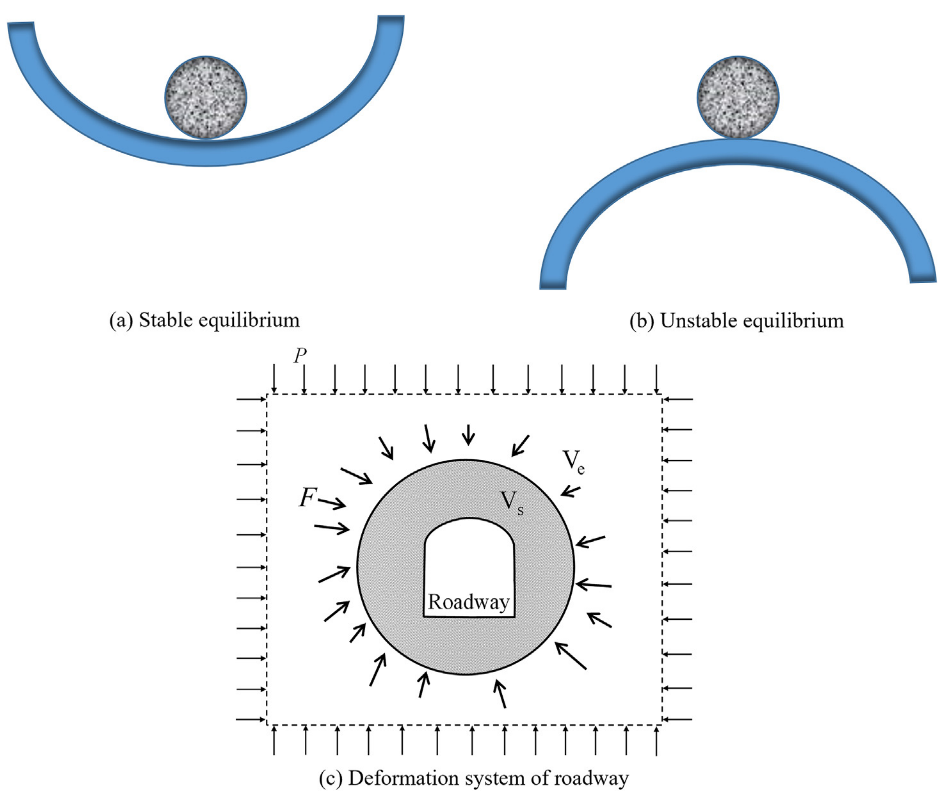

Fig. 1. Schematic diagram of stable and unstable equilibrium states.

deformation system becomes unstable subjected to mining disturbances. The coal mass in the elastic deformation area with energy storage releases energy and destroys the plastic zone and support. The remaining energy is converted into kinetic energy and rock burst occurs.

There are many factors affecting the occurrence of rock burst, but from the stability of deformation system, factors can divided the into three types, such as control variables, disturbance variables and response variables.

2.2. Variables to describe coal deformation system and it stability

Some inherent properties in a coal mass deformation system are defined as the control variables, which determine the occurrence of the rock burst. Typical control variables include the coal bursting liability index K, coal uniaxial compressive strength σ_c, coal elastic modulus E, support stress p_s and roadway radius a.

Variables acted on the boundary of the coal mass deformation system that can induce a rock burst are defined as the disturbance variables. Typical disturbance variables include in-situ stress, blasting and roof fracture. The outputs of a coal mass deformation system are defined as the response variables, including roof subsidence, roadway convergence, coal seam drilling cuttings and surrounding rock damage range. Details are presented in Table 1.

In equilibrium state, for a coal mass deformation system with plastic deformation radius ρ and the displacement u (roof subsidence or roadway convergence) under the action of the external stress P, the disturbance variable is the mining induced stress, the response variable is the size of the plastic deformation zone or the roof subsidence or roadway convergence, and the control variables are the coal uniaxial compressive strength σ_c and the bursting liability index K.

2.3. Instability criterion of coal deformation system

2.3.1. Extreme point instability criterion based on disturbance response

While a small disturbance increment ΔP is added to the external load P, the softening deformation zone expands from ρ to $\rho+\Delta\rho$, the displacement increases from u to $u+\Delta u$. If the response increment $\Delta\rho$ or Δu is limited, the system remains stable, as shown in Fig. 2. However, for a system in unstable equilibrium state, the plastic softening deformation zone or the displacement will be infinite regardless of the magnitude of the disturbance increment ΔP, that is

$$\frac{\Delta\rho}{\Delta P}=\infty, \text{or } \frac{\Delta u}{\Delta P}=\infty \tag{1}$$

2.3.2. Energy instability criterion based on disturbance response

In equilibrium state, the displacement, stress, strain, volume of plastic softening zone, and volume of other elastic zones of a coal mass deformation system under the joint action of the surface force P and volume force F are expressed as u, σ, ε, V_s, and V_e, respectively, as shown in Fig. 3.

Table 1
Variables and corresponding symbols of the coal rock deformation system.

Category of variables	Variable name	Physical quantity or symbol
Control variable	Bursting liability index of coal	K
	Uniaxial compressive strength of coal	σ_c (MPa)
	Elastic modulus of coal rock	E (MPa)
	Internal friction angle of coal	φ (°)
	Roadway radius	Roadway radius a (m)
	Support stress	Stress p_s (MPa)
Disturbance variable	in-situ and mining induced stress increment	Stress Δp (MPa)
	Blasting operation	Stress (MPa)
	Roof fracture	Displacement u (m)
Response variable	Roof subsidence	Displacement u (m)
	Roadway convergence	Displacement u (m)
	Drilling cuttings	Mass m
	Damage range of surrounding rock	Radius of plastic zone ρ (m)

A small virtual displacement Δu is applied to the coal rock mass that generates a virtual stress $\Delta\sigma$ and a virtual strain $\Delta\varepsilon$. If the virtual work done by the external force is greater than the increase of the strain energy, the system is unstable, that is,

$$\int_V F^T \Delta u \mathrm{d}v + \int_S P^T \Delta u \mathrm{d}s \geq \int_{V_e} (\sigma+\Delta\sigma)^T \Delta\varepsilon \mathrm{d}v + \int_{V_s} (\sigma+\Delta\sigma)^T \Delta\varepsilon \mathrm{d}v \tag{2}$$

where S is the total surface area, V is the total volume.

In equilibrium state, the virtual work done by the external force along the virtual displacement is equal to the virtual work done by the stress along the virtual strain,

$$\int_V F^T \Delta u \mathrm{d}v + \int_S P^T \Delta u \mathrm{d}s = \int_{V_e} (\sigma+\Delta\sigma)^T \Delta\varepsilon \mathrm{d}v + \int_{V_s} (\sigma+\Delta\sigma)^T \Delta\varepsilon \mathrm{d}v \tag{3}$$

Following equation can be obtained:

$$\int_{V_e} \Delta\sigma^T \Delta\varepsilon \mathrm{d}v + \int_{V_s} \Delta\sigma^T \Delta\varepsilon \mathrm{d}v \leq 0 \tag{4}$$

Eq. (4) shows that, the coal mass system is in unstable equilibrium state whereas the elastic deformation energy accumulated in the elastic zone is equal to the deformation energy dissipated in the plastic zone. Under the action of ΔP, the elastic deformation energy is greater than the deformation energy dissipated in the plastic zone, rock burst occurs.

3. Circular roadway rock burst formula on the disturbance response instability theory

3.1. Fundamental solution for circular roadway

The recorded rock burst events occurred in coal mines in China is 2510, of which 2178 (86.8%) occurred in roadways. The release of elastic deformation energy stored in elastic zone of surrounding rock of the roadway is key factor leading to rockburst. In practice, the cross-section of the mining roadway is rectangle, circle, trapezoid or straight wall arch. The cross-section shape other than a circular can be converted to an equivalent circle; therefore, the formula derived from a circular roadway can also be used for others by multiplying a specific coefficient (Fig. 4).

As shown in Fig. 5, a circular roadway with radius a, support stress acting on inner wall p_s and in-situ stress P at infinite, and ρ is radius of plastic zone. By ignoring the gravity and taking the unit width along the roadway axis for analysis, it can be simplified as an axisymmetric plane strain problem.

Under uniaxial compression, in the complete stress–strain curve of the specimen, the ratio of the deformation energy accumulated before the peak strength to the deformation energy consumed after the peak strength is taken as the bursting liability index of coal, as shown in Fig. 6:

$$K=\frac{A_s}{A_x} \tag{5}$$

where K is the bursting energy index, A_s is the deformation energy accumulated before the peak strength, and A_x is the deformation energy consumed after peak strength.

Ideally, the complete stress–strain curve of coal rises linearly before the peak strength, and then the strain softening curve goes down linearly after the peak strength, as shown in Fig. 7. In this case, the values of the bursting liability index be defined as formula (6).

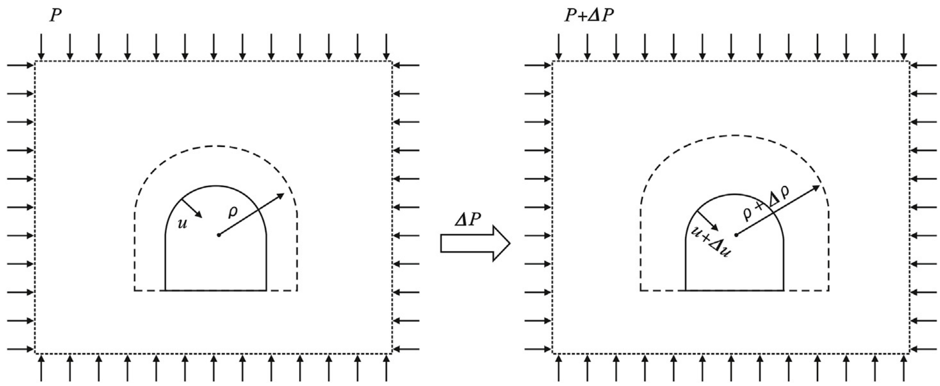

Fig. 2. Schematic diagram of disturbance response.

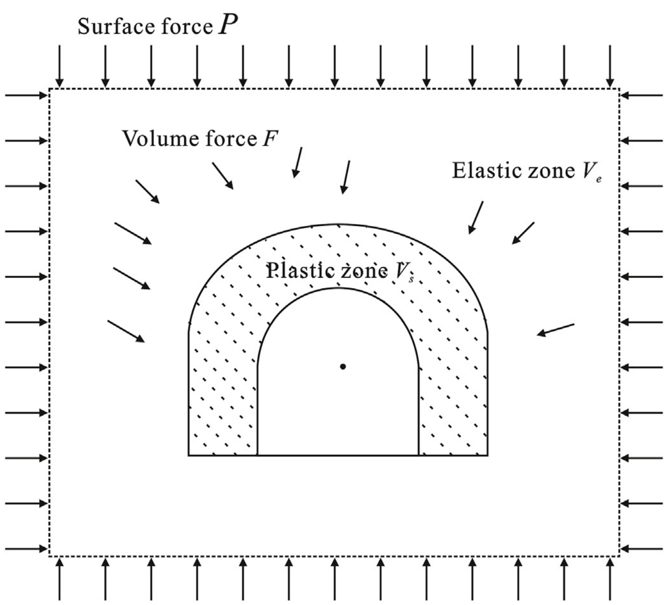

Fig. 3. Coal mass deformation system under the joint action of the surface force *P* and volume force *F*.

$$K = \frac{\lambda}{E} \tag{6}$$

where λ is the softening modulus after the peak strength of the stress-–strain curve, and *E* is the elastic modulus before the peak strength of the stress–strain curve.

In the assumption of "bilinear" constitutive relationship, the mechanical property before the peak strength is simplified to linear elasticity with modulus *E*, and the uniaxial compressive strength of coal is σ_c, and the corresponding strain is ε_c, the three parameters have relations as following.

$$E = \frac{\sigma_c}{\varepsilon_c} \tag{7}$$

It is assumed that after exceeding the peak strength, the damage variable *D* of coal is a linear isotropic damage evolution, that is, at the peak strength of coal, $D = 0$; When it reaches complete failure, $D = 1$. The one-dimensional damage evolution equation of coal under uniaxial compression is

$$\begin{aligned} &D = 0 \quad (\varepsilon < \varepsilon_c) \\ &D = \frac{\lambda}{\sigma_c}(\varepsilon - \varepsilon_c) \quad (\varepsilon \geq \varepsilon_c) \end{aligned} \tag{8}$$

The equivalent strain $\bar{\varepsilon}$ under the three-dimensional stress condition is substituted for the strain ε under the uniaxial stress condition, to obtain the damage evolution equation under the three-dimensional stress condition:

$$D = \frac{\lambda}{\sigma_c}(\bar{\varepsilon} - \varepsilon_c) \tag{9}$$

$$\bar{\varepsilon} = \sqrt{\frac{2}{9}\left[(\varepsilon_1 - \varepsilon_2)^2 + (\varepsilon_2 - \varepsilon_3)^2 + (\varepsilon_3 - \varepsilon_1)^2\right]} \tag{10}$$

Where ε_1, ε_2, and ε_3 are the principal strains. Assuming that the radial stress at the junction of the elastic zone and the softening zone is σ_r^p, the stress in the elastic zone is:

$$\sigma_r = \frac{\rho^2}{r^2}\sigma_r^p + \left(1 - \frac{\rho^2}{r^2}\right)P \tag{11}$$

$$\sigma_\theta = \frac{-\rho^2}{r^2}\sigma_r^p + \left(1 + \frac{\rho^2}{r^2}\right)P \tag{12}$$

where *r* represents the radial coordinate. Thus, the stress at the junction is:

$$\sigma_r = \sigma_r^p, \sigma_\theta = 2P - \sigma_r^p \tag{13}$$

From Eq. (11) and Eq. (12), using Hooke's law, the radial strain ε_r and tangential strain ε_θ can be obtained as following:

$$\varepsilon_r = \frac{1+\mu}{E}\left(\sigma_r^p - P\right)\frac{\rho^2}{r^2} + \frac{(1+\mu)(1-2\mu)}{E}P \tag{14}$$

$$\varepsilon_\theta = \frac{1+\mu}{E}\left(P - \sigma_r^p\right)\frac{\rho^2}{r^2} + \frac{(1+\mu)(1-2\mu)}{E}P \tag{15}$$

Where μ is Poissions ratio of coal.

The Mohr–Coulomb criterion is adopted at the junction of the plastic deformation zone and elastic zone:

$$\sigma_\theta = m\sigma_r + \sigma_c \tag{16}$$

$$m = \frac{1 + \sin\varphi}{1 - \sin\varphi} \tag{17}$$

Where, φ is internal friction angle of coal.

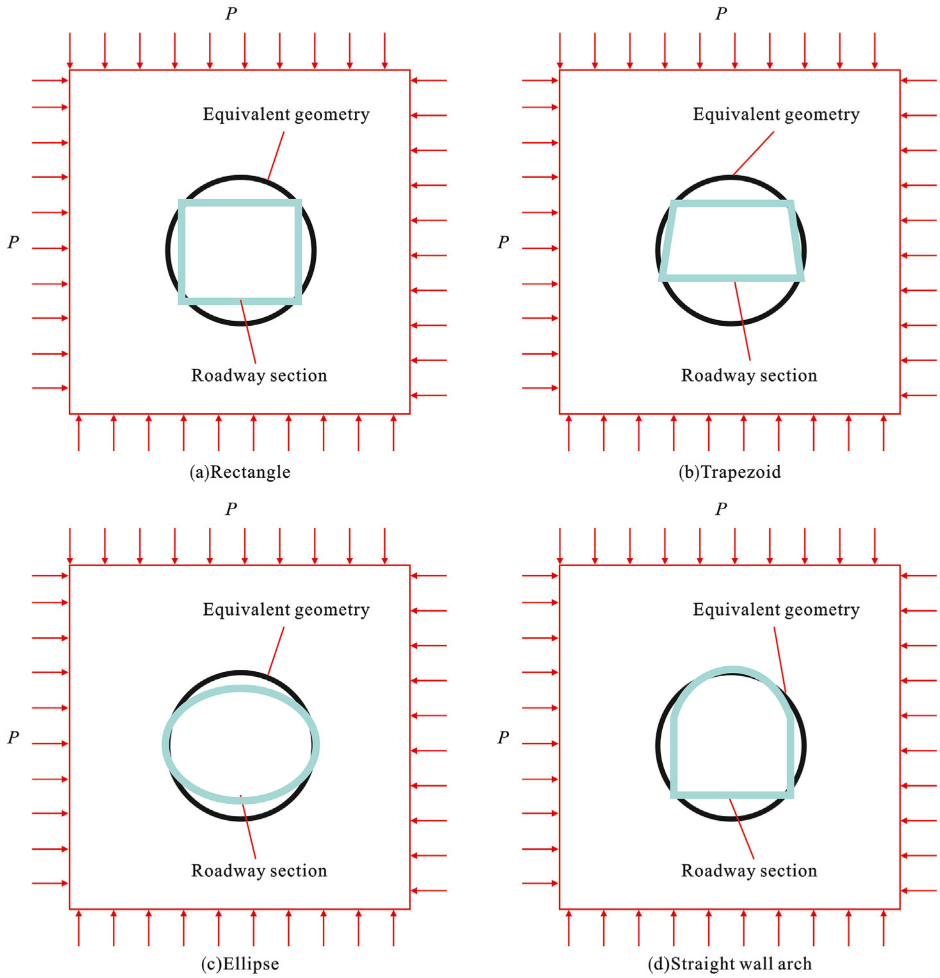

Fig. 4. Roadway cross section Simplification [26].

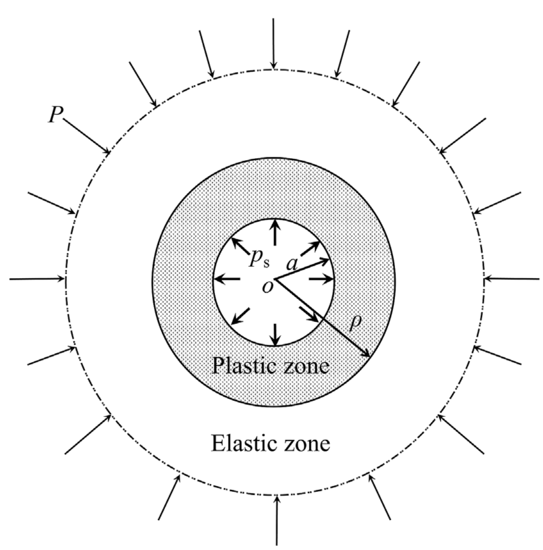

Fig. 5. Mechanical model of rock burst in circular roadway [27].

Substituting Eq. (13) into Eq. (16), it gives

$$\sigma_r^p = \frac{2P - \sigma_c}{m+1} \tag{18}$$

In the plastic zone

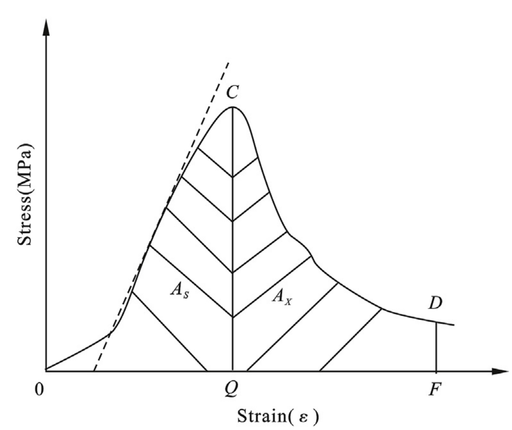

Fig. 6. Schematic of calculation of the bursting energy index.

$$\varepsilon_r = \frac{du}{dr}, \varepsilon_\theta = \frac{u}{r} \tag{19}$$

Where ε_r and ε_θ are radial strain and tangential strain respectively.

From the incompressible volume conditions in the plastic zone

$$\varepsilon_r + \varepsilon_\theta = 0 \tag{20}$$

Substituting Eq. (19) into Eq. (20), it gives

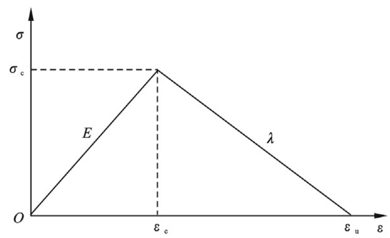

Fig. 7. Bi-linear stress–strain curve of coal rock.

$$u = \frac{B}{r}, \varepsilon_r = \frac{-B}{r^2}, \varepsilon_\theta = \frac{B}{r^2} \tag{21}$$

According to Eq. (10) the equivalent strain can be obtained:

$$\bar{\varepsilon} = \frac{2}{\sqrt{3}}\frac{B}{r^2} \tag{22}$$

Where, B is a constant. The softening zone is in three-dimensional stress state. Extending a uniaxial strain to a triaxial strain in plastic mechanics, At the junction of strain softening zone and elastic zone the equivalent strain is $\bar{\varepsilon} = \varepsilon_c$, and substituted into Eq. (22)) to obtain

$$B = \sqrt{3}\rho^2\varepsilon_c \Big/ 2 \tag{23}$$

The damage evolution equation in the softening zone can be obtained by substituting Eq. (22) and Eq. (23) into Eq. (9).

$$D = \frac{\lambda}{\sigma_c}\left(\frac{\rho^2}{r^2}\varepsilon_c - \varepsilon_c\right) \tag{24}$$

In the case of coal mass damage in plastic softening zone, the effective stress component are

$$\tilde{\sigma}_r = \frac{\sigma_r}{1-D}, \tilde{\sigma}_\theta = \frac{\sigma_\theta}{1-D} \tag{25}$$

The stress σ_r, σ_θ in the Mohr–Coulomb criterion as shown in Eq. (16) are replaced by the effective stress Eq. (25). Thus, we gotten follwing equation

$$\frac{\sigma_\theta}{1-D} = \frac{m\sigma_r}{1-D} + \sigma_c \tag{26}$$

Regardless of the volume force, equilibrium equation is:

$$\frac{d\sigma_r}{dr} + \frac{\sigma_r - \sigma_\theta}{r} = 0 \tag{27}$$

Take Eq. (26) into Eq. (27) and get following differential equation, which the radial stress σ_r in the damage zone should satisfy.

$$\frac{d\sigma_r}{dr} - (m-1)\frac{\sigma_r}{r} = \frac{\sigma_c + K\sigma_c}{r} - \frac{K\sigma_c}{r^3}\rho^2 \tag{28}$$

Combined with the boundary condition of $\sigma_r(a) = p_s$, the radial stress in plastic zone of the roadway is obtained by solving this equation:

$$\sigma_r = \left[p_s - \frac{K\sigma_c}{(m+1)}\frac{\rho^2}{a^2} + (1+K)\frac{\sigma_c}{m-1}\right]\left(\frac{r}{a}\right)^{m-1} + \frac{K\sigma_c}{(m+1)}\frac{\rho^2}{r^2} - (1+K)\frac{\sigma_c}{m-1} \tag{29}$$

According to the continuous condition of radial stress at $r = \rho$, the radial stess calculated by Eq. (18) is equal to the radial stress calcuated by Eq. (29). So we get the relationship between disturbance variable, response variable and control variable as follows:

$$\frac{P}{\sigma_c} = \frac{m+1}{2}\left[\frac{p_s}{\sigma_c} + (1+K)\frac{1}{m-1}\right]\left(\frac{\rho}{a}\right)^{m-1} - \frac{K}{2}\left(\frac{\rho}{a}\right)^{m+1} - (1+K)\frac{1}{m-1} \tag{30}$$

where P disturbance variable is the stress of the coal mass deformation system in a circular roadway; control variable σ_c, K, m, and a and p_s are the coal uniaxial compressive strength, coal bursting energy index, coal material constant, and roadway radius and support stress, respectively; Response variable ρ is the radius of the plastic softening zone of a circular roadway.

3.2. Formula of roadway rock burst by extreme point instability criterion

Using the disturbance response criterion Eq. (1) the critical radius ρ_{cr} for roadway rock burst occurrence is obtained:

$$\frac{\rho_{cr}}{a} = \sqrt{1 + \frac{1}{K} + \frac{1}{K}(m-1)\frac{p_s}{\sigma_c}} \tag{31}$$

If the support stress is not considered, $p_s = 0$, the critical radius strain softening zone ρ_{cr} of the rock burst is as follows:

$$\frac{\rho_{cr}}{a} = \sqrt{1 + \frac{1}{K}} \tag{32}$$

Substituting Eq. (32) into Eq. (30), the critical stress P_{cr} of the roadway rock burst is obtained:

$$\frac{P_{cr}}{\sigma_c} = \frac{1}{m-1}\left\{K\left[1 + \frac{1}{K} + \frac{1}{K}(m-1)\frac{p_s}{\sigma_c}\right]^{\frac{m+1}{2}} - K - 1\right\} \tag{33}$$

In general, the internal friction angle is $\varphi = 30°$; thus, the critical stress P_{cr} of the rock burst is

$$P_{cr} = \frac{\sigma_c}{2}\left(1 + \frac{1}{K}\right)\left(1 + \frac{4p_s}{\sigma_c}\right) + \frac{2p_s^2}{K} \tag{34}$$

In general contiton, the last item in above equation is smaller, neglect it and obtain:

$$P_{cr} = \frac{\sigma_c}{2}\left(1 + \frac{1}{K}\right)\left(1 + \frac{4p_s}{\sigma_c}\right) \tag{35}$$

If the support stress is not considered, i.e., $p_s = 0$, the critical stress P_{cr} of rock burst is

$$P_{cr} = \frac{\sigma_c}{2}\left(1 + \frac{1}{K}\right) \tag{36}$$

From the established instability theory of disturbance response for rock burst, rock burst is instability of the coal mass deformation system with the infinit deformation response. If the system is in an unstable equilibrium state, the system will be unstable regardless of the disturbance increment size. Accordingly, the analytical solution of rockburst in circular roadway is derived. It is found that there is a critical index for the coal deformation system. There is a critical index for the stress on the surrounding rock of the roadway. When the loads on the roadway exceeds the critical stress, the system loses stability under external disturbance. These critical stress is determined from coal uniaxial compressive strength, bursting energy index, roadway radius and roadway support stress. Therefore, the monitoring and prevention of rock burst can be carried out accordingly.

3.3. Formula of roadway rock burst by energy criterion instability

In the elastic zone of roadway as shown in Fig. 3. Select the radius of strain softening zone ρ as a state variable, strain increment in the elastic zone by Eq. (14) and Eq. (15) can be obtained when $\Delta\rho$ increment is extend to roadway deformation system:

$$\Delta\varepsilon_r = \frac{1+\mu}{E}\left(\sigma_r^p - P\right)\frac{2\rho\Delta\rho}{r^2} \tag{37}$$

$$\Delta\varepsilon_\theta = \frac{1+\mu}{E}\left(P - \sigma_r^p\right)\frac{2\rho\Delta\rho}{r^2} \tag{38}$$

From Eq. (11) and Eq. (12), The stress increment in the elastic zone is

$$\Delta\sigma_r = \frac{2\rho\Delta\rho}{r^2}\sigma_r^p - \frac{2\rho\Delta\rho}{r^2}P = \frac{2\rho\Delta\rho}{r^2}\left(\sigma_r^p - P\right) \tag{39}$$

$$\Delta\sigma_\theta = -\frac{2\rho\Delta\rho}{r^2}\sigma_r^p + \frac{2\rho\Delta\rho}{r^2}P = \frac{2\rho\Delta\rho}{r^2}\left(P - \sigma_r^p\right) \tag{40}$$

The increment in the strain energy stored in the elastic zone is

$$\begin{aligned}\Delta W_e &= \int_0^{2\pi}\int_\rho^\infty (\Delta\sigma_r\Delta\varepsilon_r + \Delta\sigma_\theta\Delta\varepsilon_\theta) r\mathrm{d}r\mathrm{d}\theta \\ &= 8\pi\frac{1+\mu}{E}\left[\frac{(m-1)P+\sigma_c}{m+1}\right]^2(\Delta\rho)^2\end{aligned} \tag{41}$$

From Eq. (19) and Eq. (24), The strain increment in the softening zone is

$$\Delta\varepsilon_r = -\frac{\sqrt{3}}{2}\varepsilon_c 2\rho\frac{\Delta\rho}{r^2} = -\sqrt{3}\varepsilon_c\rho\frac{\Delta\rho}{r^2} \tag{42}$$

$$\Delta\varepsilon_\theta = \frac{\sqrt{3}}{2}\varepsilon_c 2\rho\frac{\Delta\rho}{r^2} = \sqrt{3}\varepsilon_c\rho\frac{\Delta\rho}{r^2} \tag{43}$$

From Eq. (26) and Eq. (29), The stress increment in the softening zone is

$$\Delta\sigma_r = -\frac{\lambda\sigma_c}{E(m+1)}\cdot\frac{2\rho\Delta\rho}{a^2}\cdot\left(\frac{r}{a}\right)^{m-1} + \frac{\lambda\sigma_c}{E(m+1)}\cdot\frac{2\rho\Delta\rho}{r^2} \tag{44}$$

$$\Delta\sigma_\theta = -\frac{m\lambda\sigma_c}{E(m+1)}\cdot\frac{2\rho\Delta\rho}{a^2}\cdot\left(\frac{r}{a}\right)^{m-1} - \frac{\lambda\sigma_c}{E(m+1)}\cdot\frac{2\rho\Delta\rho}{r^2} \tag{45}$$

The increment in the strain energy stored in the softening zone is

$$\Delta W_s = \int_0^{2\pi}\int_a^\rho (\Delta\sigma_r\Delta\varepsilon_r + \Delta\sigma_\theta\Delta\varepsilon_\theta) r\mathrm{d}r\mathrm{d}\theta = \left[\frac{1}{\rho^2} - \frac{\rho^{m-1}}{a^{m+1}}\right]\cdot\frac{4\sqrt{3}\pi K\sigma_c^2}{E(m+1)}\rho^2\Delta\rho^2 \tag{46}$$

The condition for the occurrence of a rock burst from the energy perspective is

$$\int_{V_e}\Delta\sigma^T\Delta\varepsilon \mathrm{d}v + \int_{V_s}\Delta\sigma^T\Delta\varepsilon \mathrm{d}v \le 0 \tag{47}$$

Therefore,

$$8\pi\frac{1+\mu}{E}\left[\frac{(m-1)P+\sigma_c}{m+1}\right]^2\frac{1}{\rho^2} + \left[\frac{1}{\rho^2} - \frac{\rho^{m-1}}{a^{m+1}}\right]\cdot\frac{4\sqrt{3}\pi K\sigma_c^2}{E(m+1)} \le 0 \tag{48}$$

Using Eq. (28) the continuous condition of radial stress at $r = \rho$, the equation about ρ/a can be obtained

$$\begin{aligned}\frac{\sqrt{3}}{2}\frac{m+1}{1+\mu}K\left[\left(\frac{\rho}{a}\right)^{m+1} - 1\right] = \Bigg[&\frac{(m+1)}{2}\left[\frac{(m-1)p_s}{\sigma_c} + (1+K)\right]\left(\frac{\rho}{a}\right)^{m-1} \\ &- \frac{m-1}{2}K\left(\frac{\rho}{a}\right)^{m+1} - K\Bigg]\end{aligned} \tag{49}$$

Eq. (49) cannot get the explicit solution, however it very easy to get numerical solution. The critical stress P_{cr} can be obtained by substituting numerical solution into Eq. (30).

3.4. Comparison between two rock burst instability criterion

Combined with the above theories, the critical stress of rockburst P_{cr} is calculated by extreme point and energy methods, respectively, for variables K and σ_c, as shown in Fig. 8. While the variable K in the (0, 1) interval, the max error of two methods is 3%, While the variable K in the (1, ∞) interval, the two result are very close, the max error of two methods is 0.5%. When the variable is σ_c, the extreme point formula function curve and energy function curve are proportional curves, the values are very close, as shown in Fig. 9.

3.5. Critical index of rock burst occurrence

3.5.1. Critical stress

Based on the disturbance response instability theory of rockburst, the analytical solution of rock bursts in circular roadways was derived, and the critical index of the coal mass deformation system was obtained (Eq. (32)). When the stress in the surrounding rock is greater than the critical stress, rock burst occurs. The critical index is determined by the coal

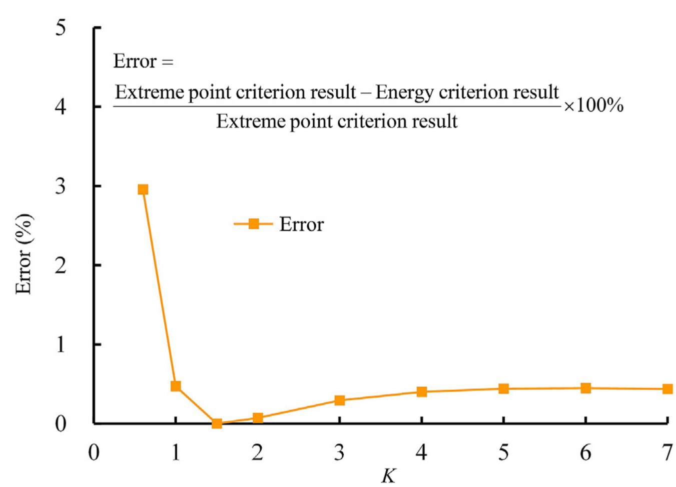

Fig. 9. Error of two methods.

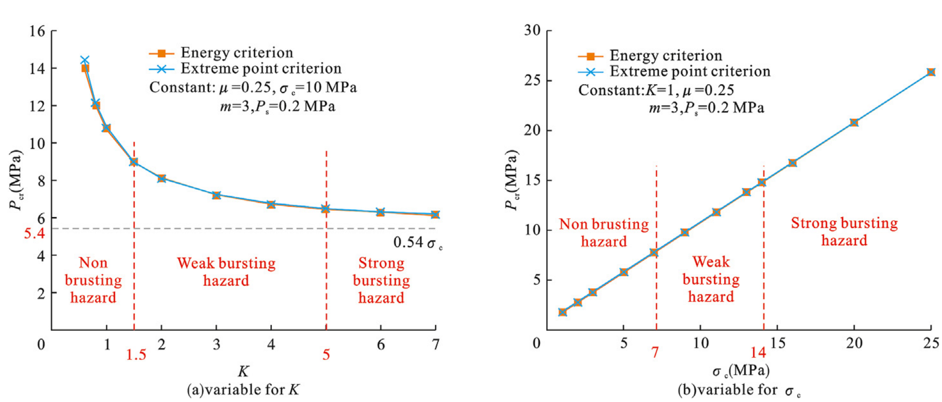

Fig. 8. Comparison between theoretical formula of rockburst by two criterion.

uniaxial compressive strength, bursting energy index, roadway radius, and roadway support stress. Therefore, the monitoring and early warning of rock bursts can be realized through the comparison of the monitored in-situ stress and the critical stress. In the prevention and control of rock bursts, the stress of the coal mass around the roadway can be controlled; on the other hand, the coal uniaxial compressive strength, bursting energy index, roadway radius, and roadway support stress can also be controlled, so that the stress of the surrounding rock is less than the critical stress of the rock burst.

3.5.2. Critical radius of plastic softening zone

The critical radius of the plastic softening zone refers to the radius of plastic softening of boundary in the surrounding rock when the critical condition is reached. Meanwhile, after the rock burst is started, the coal rock mass in the plastic softening zone can absorb the bursting energy. Therefore, the critical radius of the plastic softening zone can be used as an important indicator for monitoring and early warning of rock bursts. The critical radius ρ_{cr} of the roadway rock burst is shown in Eq. (31).

3.5.3. Critical energy

According to dominant energy storage and release, rock bursts can be divided into three types [28]: energy storage and release by coal mass (coal compression type), energy storage and release by the roof (roof tension type), and energy storage and release by fault and surrounding rock (fault shear type). Their stored energies are different when they reach the instability condition. The equations of the energy released by three types rock bursts in the critical state are as follows.

(1) Coal compression type rock burst

When the rock burst occurs, the energy stored in the elastic zone is released rapidly. Part of the energy is used to damage the coal mass in the softening area, and the remaining energy is expressed in the form of rock burst. Therefore, the calculated energy storage in the elastic zone in the critical state can be used to estimate the magnitude of the rock burst.

The strain in the elastic zone due to roadway excavation is:

$$\varepsilon_r = \frac{1+\mu}{E}\frac{(1-m)P-\sigma_c}{m+1}\frac{\rho^2}{r^2}, \varepsilon_\theta = \frac{1+\mu}{E}\frac{(m-1)P+\sigma_c}{m+1}\frac{\rho^2}{r^2} \tag{50}$$

The strain energy stored in the elastic zone is

$$W = \int_0^{2\pi}\int_\rho^\infty \left(\frac{1}{2}\sigma_r\varepsilon_r + \frac{1}{2}\sigma_\theta\varepsilon_\theta\right) r\mathrm{d}r\mathrm{d}\theta = \pi\frac{1+\mu}{E}\left[\frac{(m-1)P+\sigma_c}{m+1}\right]^2\rho^2 \tag{51}$$

In the critical state, $\frac{\rho_{cr}}{a} = \sqrt{1+\frac{1}{K}}$, and the released energy W in one unit length roadway is

$$W = \frac{(1+\mu)\pi a^2\sigma_c^2}{16E}\left(\frac{1}{K}+1\right)\left(\frac{1}{K}+2\right)^2 \tag{52}$$

(2) Roof tension type rock burst

Similarly, according to the disturbance response instability theory, the released energy W with the critical goaf span of L_{cr} is

$$W = \frac{bp^2\left(3L_{cr}^5 + 10\chi L_{cr}^3 + 120\chi^2 L_{cr}\right)}{160Eh_1{}^3} \tag{53}$$

$$\chi = \frac{L_{cr}\left(\alpha^2L_{cr}^2 + 6\alpha L_{cr} + 12\right)}{3\alpha(\alpha L_{cr}+2)}, b = b_0 - 2d\cot\beta, \alpha = \sqrt[4]{\frac{3\eta}{Eh_1{}^3}}$$

where p is the load and self-weight of the overburden of the roof, kN; b_0 is the length of the working face, m; d is the distance between the roof and the coal seam, m; β is the fracture angle of the overburden, °; h_1 is the thickness of the roof, m; E is the elastic modulus of the roof rock, MPa; and η is the stiffness coefficient of the coal seam.

(3) Fault shear type rock burst

Similarly, according to the disturbance response instability theory, the released energy W in the critical state is:

$$W \approx \frac{zh_2G\left[(S_1-u_1)^2 - (S_2-u_2)^2\right]}{2X} \tag{54}$$

where z is the effective length of the strike of the slip fault, m; h_2 is the fault throw, m; G is the shear modulus of the rock in the fault zone, MPa; S_1 and S_2 are the far-field shear displacement before and after the fault slip, respectively, m; u_1 and u_2 are the shear displacement before and after the slip of the fault zone, respectively, m; and $2X$ is the width of fault surrounding rock, m.

The essence of a rock burst is that after the released energy is dissipated by the surrounding rock and support, the remaining energy is converted into the rock burst kinetic energy. Therefore, the prevention and control of a rock burst aims at absorbing the energy released by the rock burst and design of the support.

3.6. Relationship between bursting liability index and critical stress

The main control variables of rock bursts are the bursting liability index K, uniaxial compressive strength σ_c, the elastic modulus E and the internal friction angle φ. Among them, the uniaxial compressive strength σ_c, the elastic modulus E, and the internal friction angle φ can be obtained through standard tests. The values of the bursting liability index and the bursting energy index are the same, and they reflect the energy release capability of the coal mass when the bursting occurs.

The relationship between the bursting liability index and the critical stress of rock bursts of 60 coal mines in China is shown in Fig. 10. It can be observed that the bursting liability index of coal seams is roughly from 0.8 to 7.5. In other words, with decrease of the bursting liability index, the critical stress of the rock burst increase and the risk of the rock burst decreases, and vice versa.

4. Rock burst hazard evaluation based on the disturbance response instability theory

4.1. Hazard evaluation of rock burst based on stress

Rock burst hazard evaluation refers to the prediction of risk and rock

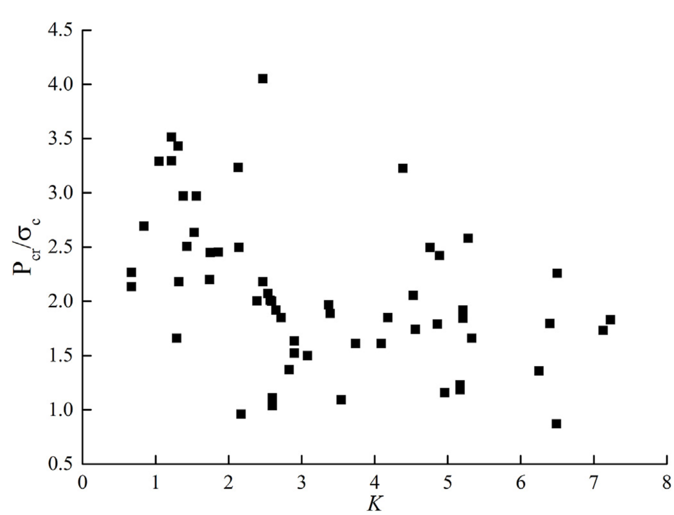

Fig. 10. Relationship between the bursting liability index and critical stress of rock bursts in coal mines in China.

burst range before mining, which can be used as a guide for the prevention and control of rock bursts.

The disturbance response instability theory gives the critical stress P_{cr} of the rock burst. By comparing the measured in-situ stress with the critical stress P_{cr}, the evaluation criterion of rock burst hazard can be proposed as follows:

$$W_P = \frac{P}{nP_{cr}} \tag{55}$$

where W_P is the stress index; P is the in-situ stress of coal in the area to be evaluated, MPa; $P = \xi\gamma h$, MPa; ξ is the concentration coefficient of mining or tectonic stress, which is determined according to mining and geological conditions, generally taking 1.2–3.0; γ is the average unit weight of the overburden, 25 kN/m^3; h is the buried depth of the coal seam, m; P_{cr} is the critical stress obtained by theoretical calculation, MPa; and n is the correction coefficient related to the uniaxial compressive strength of coal material.

$$n = 1.63 + 22.09 \times 0.80^{\sigma_c} \tag{56}$$

According to the relative magnitude of the in-situ stress and critical stress, the rock burst hazard can be divided into several levels. According to Eq. (55), as the stress of the coal mass increases, the stress index goes up, and the rock burst hazard level increases. Therefore, according to the ratio (stress index) of the stress of the coal mass to the critical stress of the rock burst, the rock burst hazard level in different mining sections can be obtained. Table 2 lists the rock burst hazard level and classification standard based on the stress index.

For example, 305 working face in a mine, as shown in Fig. 11. The west of the 305 working face is the 303 working face (to be mined), and the other directions are solid coal. The lengths of the maingate, tailgate and open-cut of the 305 working face are 2310 m, 2110 m, and 250 m, respectively. The average thickness of the coal seam is 7 m, the average dip angle of the coal seam is 10°, and the average buried depth of the working face is 1050 m. The cross-section of the roadway is rectangular, with a width of 5.4 m and a height of 3.5 m. The roadway is supported with rebar bolt, cable and metal mesh (Table 3). According to the assessment results of the coal seam bursting liability of the mine, the coal uniaxial compressive strength is 10.17 MPa, and the bursting energy index is 0.84.

The stress index method is used to evaluate the rock burst hazard during the excavation of the roadways of the 305 working face. The specific steps are as follows [29]:

(1) The uniaxial compressive strength of the coal seam is 10.17 MPa, and the bursting energy index is 0.84.
(2) The support stress is calculated according to the roadway support parameters. In one unit length of the roadway, there are 7 anchor bolts and 3 anchor cables. The support stress is:

$$p_s = \frac{7 \times 180\ \text{kN} + 3 \times 450\ \text{kN}}{1\ \text{m} \times 5.4\ \text{m}} = 0.48\ \text{MPa}$$

(3) The rock burst critical stress is calculated according to Eq. (35): $P_{cr} = 51.77$ MPa.

Table 2
Hazard level and classification standard of rock bursts based on the stress index.

rock burst hazard level	Stress index W_P
No rock burst hazard	$0 < W_P < 0.25$
Weak rock burst hazard	$0.25 \le W_P < 0.5$
Medium rock burst hazard	$0.5 \le W_P < 0.75$
Strong rock burst hazard	$W_P \ge 0.75$

(4) Table 4 presents the occurrences of rock bursts in the mine.
(5) The hazard level and classification standard of rock bursts evaluated by stress index are taken from Table 2.
(6) Taking the tailgate of the 305 working face as an example, the actual stress of coal is calculated. According to the geological conditions of the 305 working face, the coal mass stress of the roadway mainly includes the stress of the overburden and the structural stress generated by the fault. The roadway is 2110 m in length with an average buried depth of 1050 m. The overburden unit weight γ of the coal seam is 25 kN/m^3, and the self-weight stress σ_z is

$$\sigma_z = \gamma h = 26.25\text{MPa}$$

At the fault, the coal rock stress is mainly structural stress. A stress rise zone is formed near the fault. According to the method in Ref. [13], the actual coal seam stress distribution of the maingate, tailgate and open-cut of the 305 working face is calculated undertaken consideration of overburden stress and structural stress of the fault.

(7) According to Eq. (55) and the actual coal mass stress of the tailgate obtained in step (6), the stress index of the tailgate, maingate, and open-cut can be calculated.
(8) The critical stress indexes of the maingate, tailgate and open-cut are compared with the rock burst hazard levels and classification standards provided in Table 2 to determine the rock burst hazard level of the roadways. The rock burst hazard areas are plotted on the mining plan of the 305 working face based on the stress index method, as shown in Fig. 12.

4.2. Risk evaluation of rock burst based on energy

The maximum energy released by a rock burst roadway is W_{max}. The residual bursting energy is W_{sur} after the surrounding rock dissipates energy W_c. The energy absorption capacity of the support is W_{sup}. From the perspective of energy, the energy safety coefficient N_e of the roadway support is defined as follows:

$$N_e = \frac{W_{sup}}{W_{max} - W_c} = \frac{W_{sup}}{W_{sur}} \tag{57}$$

When $N_e > 1$, the energy absorbed by the support is greater than the residual bursting energy of the roadway, the rock burst hazard is relatively small; when $N_e < 1$, the rock burst hazard is relatively large.

Fine sandstone with an average thickness of 54.7 m exists in the overburden of the working face 305 with an average distance of 16.3 m from the coal seam. The adjacent working face has experienced a roof high-energy event, and the risk of roof type rock burst is high. The coal seam has a strong bursting liability. A coal compression type rock burst occurred in 303 working face, thus, the possibility of a coal compression type rock burst is also great.

(1) Energy release

Taking the radius of the circumcircle of the rectangular roadway as the equivalent radius, a is 3.2 m, Poisson's ratio μ is 0.28, and the elastic modulus is 2.11 GPa. The total strain energy released by the coal type rock burst in the roadway per unit length is 7.59E+06 J according to Eq. (52). The elastic modulus of roof rock is 7 GPa, and the load is 1.1 MPa. The total strain energy released by the roof is 7.35E+08J according to Eq. (53).

(2) Energy loss

According to Ref. [30], 10% of the energy released is converted into vibrating wave energy, then the maximum theoretical released energy

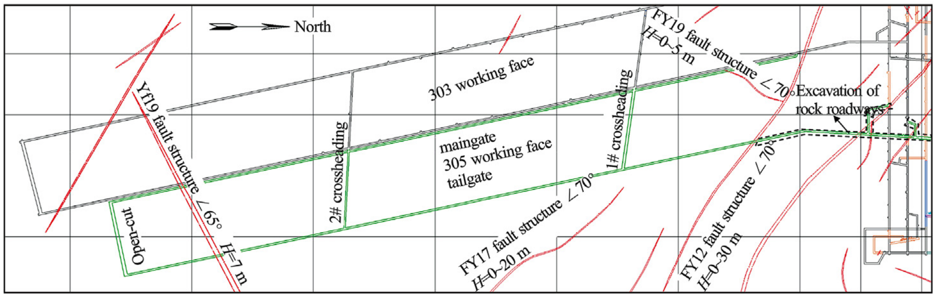

Fig. 11. Schematic of the 305 working face.

Table 3
Support parameters of the 305 working face in last few years.

Supporting materials	Row spacing (m)	Spacing (m)	Quantity per unit length	Supporting force (kN)
Bolt	1.0	0.8	7	180
Cable	1.0	2.0	3	450

Table 4
Occurrence of rock bursts in the mine.

Location	Buried depth (m)	Overburden stress (MPa)	Stress concentration factor ξ	Approximate actual stress (MPa)
Connecting roadway and crossroad in the mining area	870	21.75	Affected by other roadway and faults, 1.4 is assumed	28.28
Advance of working face 301	940	23.63	Affected by abutment pressure, 1.5 is assumed	35.45
Mining roadway of 303 working face	1070	26.75	Affected by the abutment pressure and dual heading faces, 1.4 is assumed	37.45

$W_{\max}$ of the coal compression type rock burst is 7.59E+05 J and the maximum theoretical released energy $W_{\max}$ of the roof type rock burst is 7.35E+07 J.

Considering the worst situation, the transmission attenuation energy of the coal compression type rock burst is 0 J. For the roof tention type rock burst, the energy released in the first roof caving is the largest, which has the greatest impact on the working face. The energy absorption coefficient ς of the goaf is determined as 0.009 according to the field microseismic data. The transmission attenuation energy is 7.3E+07 J. Energy consumption in the plastic zone per unit length in the roadway in the critical state can be obtained Eq. (53) as $W_c = 46.13$ kJ/m^2.

According to the materials used for roadway support, it is determined that each anchor bolt can absorb energy of 30 kJ, each anchor cable can absorb energy of 70 kJ, each hydraulic support can absorb energy of 479.6 kJ, and the metal mesh can absorb energy of 3.1 kJ/m^2. Thus, the energy absorption of the support is $W_{sur} = 71.58$ kJ/m^2. Substituting into Eq. (57), the energy safety coefficient corresponding to each type of rock burst can be obtained: for the coal type rock burst $N_e = 3.1$, and for the roof type rock burst $N_e = 1.6$. The minimum energy safety coefficient is that of the roadway, that is, the energy safety coefficient of the auxiliary transportation channel is 1.6.

5. Monitoring and warning of rock burst based on the disturbance response instability theory

5.1. Technical system for monitoring and early warning of rock burst

The disturbance response instability theory gives the critical index of rock burst. Its value reflects the risk of rock burst in the coal rock deformation system. Rock burst is often accompanied by changing of the response variables of the coal rock deformation system such as roof subsidence, roadway convergence, drilling cuttings, support stress, acoustic signal of coal rock deformation and fracture, electrical signal, and magnetic signal. By comparison of the measured mining induced stress in the surrounding rock with the critical mining induced stress of rock burst, the rock burst hazard level can be identified in real time. If burst risk is high, corresponding measures should be undertaken. Mining activities can only be conducted after the index is less than the critical warning value. The monitoring and early warning system of rock bursts is shown in Fig. 13.

5.2. Stress monitoring

5.2.1. Monitoring of mining-induced stress

The measurement of mining induced stress can be realized through various types of measuring instruments, such as pressure sensors, pressure pillows, stress gauges, etc. According to the disturbance response instability theory, the mining-induced stress is a disturbance variable, and it reflects the stability of the coal rock mass deformation system. The rock burst risk level can be judged by comparing the actual mining-induced stress with its critical value. According to the relative magnitude of the mining-induced stress and its critical value, the rock burst risk can be divided into several levels.

The peak mining-induced stress in the surrounding rock is the maximum tangential stress in the elastic zone. Therefore, according to the boundary conditions of the elastic zone $r = \rho$, the maximum tangential stress $\sigma_{\theta\ \max}$ can be obtained form Eq. (13) and Eq. (16).

$$\sigma_{\theta\ \max} = 2P\frac{m}{m+1} + \frac{\sigma_c}{m+1} \tag{58}$$

The mining-induced stress concentration coefficient of the surrounding rock of the roadway ξ can be obtained as follows:

$$\xi = \frac{\sigma_{\theta\ \max}}{P} = \frac{2m}{m+1} + \frac{\sigma_c}{P(m+1)} \tag{59}$$

$$\xi_{\max} = \frac{2m}{m+1} + \frac{\sigma_c}{P_{cr}(m+1)} \tag{60}$$

Therefore, the early warning of rock burst can be realized based on the monitored mining-induced stress. For example, in the mining operation process of the 303 working face, the mining-induced stress changes at 169#, 170#, 173#, and 174# measuring stations in air return

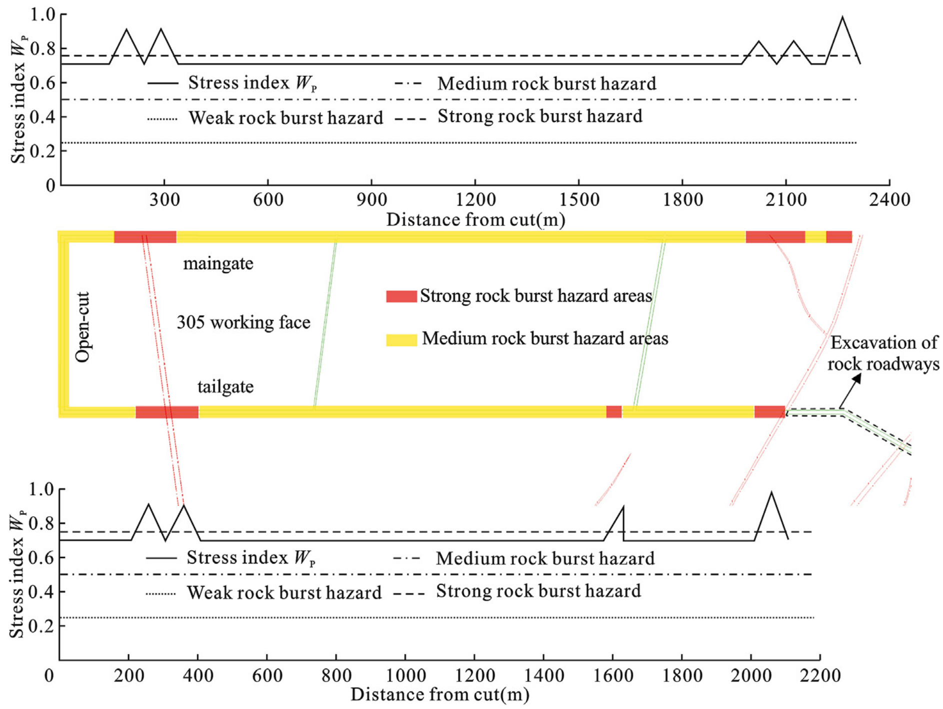

Fig. 12. Classification of rock burst hazard of the 305 working face based on the stress index method.

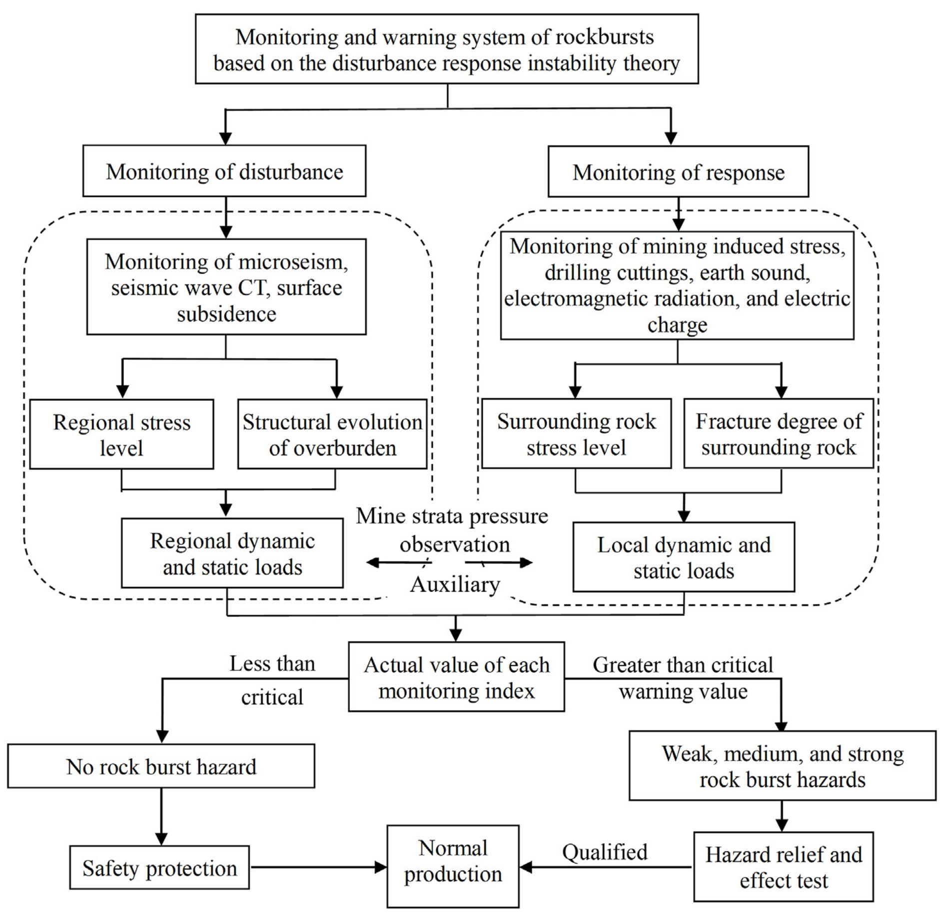

Fig. 13. Monitoring and early warning system of rock burst based on the disturbance response instability theory.

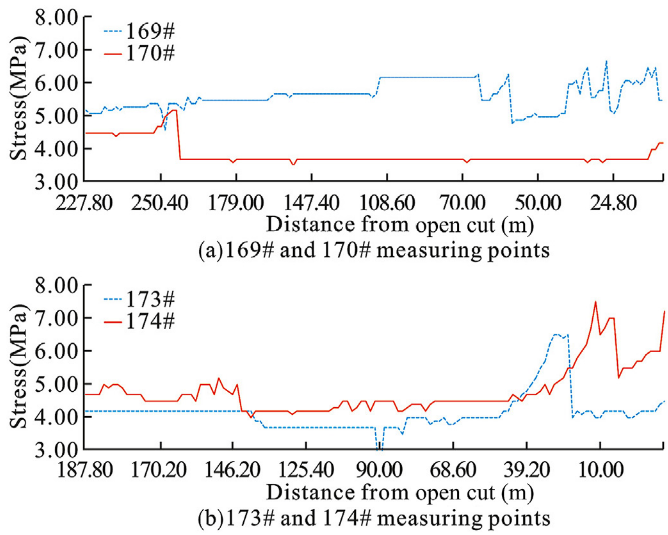

Fig. 14. Stress curves of mining-induced stress measuring points of the mine.

roadway are shown in Fig. 14 (odd number indicates shallow points and even number indicates deep points). Affected by the mining-induced stress, the stress at the 169# measuring point starts to increase approximately 180 m away from the working face, and reaches critical warning value 30–40 m from the working face. After the prevention measures, the stress is reduced to the safe value. When the 173# and 174# measuring points are approximately 50 m away from the working face, the stress starts to increase gradually and reaches the critical warning value approximately 25 m and 10 m away from the working face, respectively. After the treatment, the stress value decreases to the safe value.

5.2.2. *Drilling cutting method*

In the drilling cutting method, small-diameter holes are drilled into the coal mass and the powder discharge per unit hole depth is monitored during the drilling process. According to the disturbance response instability theory, the amount of drilling cuttings is a response variable of the coal rock deformation system. Based on the critical amount of drilling cuttings when a rock burst occurs, the rock burst hazard can be judged by comparing the monitored amount of drilling cuttings with the critical value. According to the relative magnitude of the monitored value and the critical value, the hazard can be divided into several levels. In addition, there is a quantitative relationship between the amount of pulverized coal drilled and the stress state of the coal mass. When the stress state is different, the amount of drilling cuttings in the borehole is also different. When the amount of drilling cuttings per unit length increases or exceeds the critical value, it means that the concentration of stress increases and the rock burst hazard increases.

5.3. *Energy monitoring*

5.3.1. *Monitoring for released energy*

While a coal rock mass system is damaged, energy generated by the damage propagates in the form of waves, which can be received by sensors embedded in the coal rock mass. This method is called the microseismic monitoring method. Microseismic monitoring is a regional prediction method. According to the disturbance response instability theory of rock bursts, microseisms are a response variable of the coal rock deformation system, reflecting the stability state of the coal rock deformation system. Comparing the monitoring value with the critical value, the stability of the coal rock deformation system, the rock burst hazard can be judged. The rock burst hazard can also be divided into several levels according to the relative magnitude of the monitoring value and the critical value.

Reference [30] presents a method to determine the maximum allowable mining-induced stress. The maximum allowable disturbance σ_{bmax} is the disturbance dynamic load increment that needs to be superimposed to reach the critical in-situ stress P_{cr} under the current stress P. It represents the capability of the roadway to resist the disturbance and maintain stability in a certain stress environment. To quantify the roadway resistance to a dynamic load disturbance in a specific stress environment, taking into account the low-frequency stress waves and the "incremental loading" effect of the disturbance stress and in-situ stress, the disturbance stress of coal σ_b and in-situ stress P are treated by the equivalent increment method, that is, the dynamic stress of coal is equivalent to the in-situ stress increment. The maximum allowable disturbance stress is

$$\sigma_{bmax} = \psi(P_{cr} - P) \tag{61}$$

In the equation, ψ is the nonuniform superposition coefficient of dynamic stress, which is affected by the geological and mining conditions of the working face. It is generally selected as 0.75–0.95 in engineering practice. Furthermore, The following formula can be obtained according to the relationship between dynamic stress σ_b of coal rock and particle velocity v.

$$\sigma_b = \rho_c c v \tag{62}$$

where $\rho_c c$ is the characteristic impedance of the coal, ρ_c is the coal density, which is generally 1.32–1.35 g/cm^3, and c is the velocity of the longitudinal wave.

Combining the particle peak velocity v suggested by McGarr [31], and the relationship $\lg Rv = 3.95 + 0.57M_L$ between the distance R from the focal to the source point and the rock burst intensity M_L, The maximum value of disturbance amplitude within a limited range M_{Lmax} of the roadway under certain conditions is obtained. The actual monitored microseismic magnitude is compared with the maximum allowable disturbance magnitude M_{Lmax} for rock burst warning.

5.3.2. *Monitoring of absorbed energy*

When a rock burst occurs in a roadway, the energy stored in the elastic zone of the surrounding rock is released rapidly. Part of the energy is used to destroy the coal mass in the softening and crushing zones, and the rest is in the form of residual bursting energy of the rock burst, which damages the support, as shown in Fig. 15.

When a rock burst occurs, the critical softening zone hinders its development by absorbing the released elastic energy. Thus, the softening zone also becomes the resistance zone. The absorbed energy of the rock burst can be monitored by monitoring the radius of the plastic zone.

After energy enters into plastic zone, it deforms and damages the coal in the softening zone, consuming the transmitted energy. It is assumed that when the rock burst occurs, all the coal mass in the plastic zone is damaged, and thus the residual strength is zero and all the energy consumed is used to generate new surface energy. Then, the consumed energy W_s by the coal in the plastic zone of the surrounding rock per unit length is

$$W_s = -\int_0^{2\pi}\int_a^{\rho}\frac{r}{2}(\sigma_\theta\varepsilon_\theta + \sigma_r\varepsilon_r)\mathrm{d}r\mathrm{d}\theta$$

$$= \frac{\sqrt{3}\pi\rho^2\sigma_c^2}{8E}\left[K\left(\frac{\rho}{a}\right)^4 - 2(K+1)\left(\frac{\rho}{a}\right)^2 + K + 2\right] \tag{63}$$

where σ_θ and ε_θ are the tangential stress and strain in the plastic zone, respectively, and σ_r and ε_r are the radial stress and strain in the plastic zone, respectively.

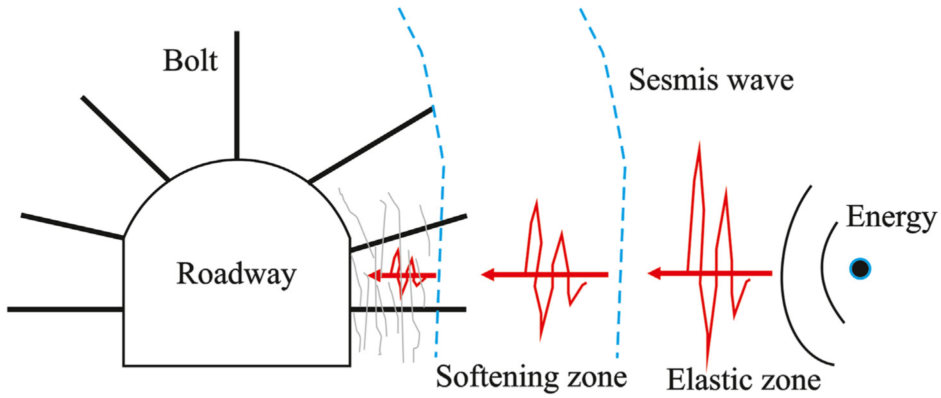

Fig. 15. Process of energy transmission during the rock burst.

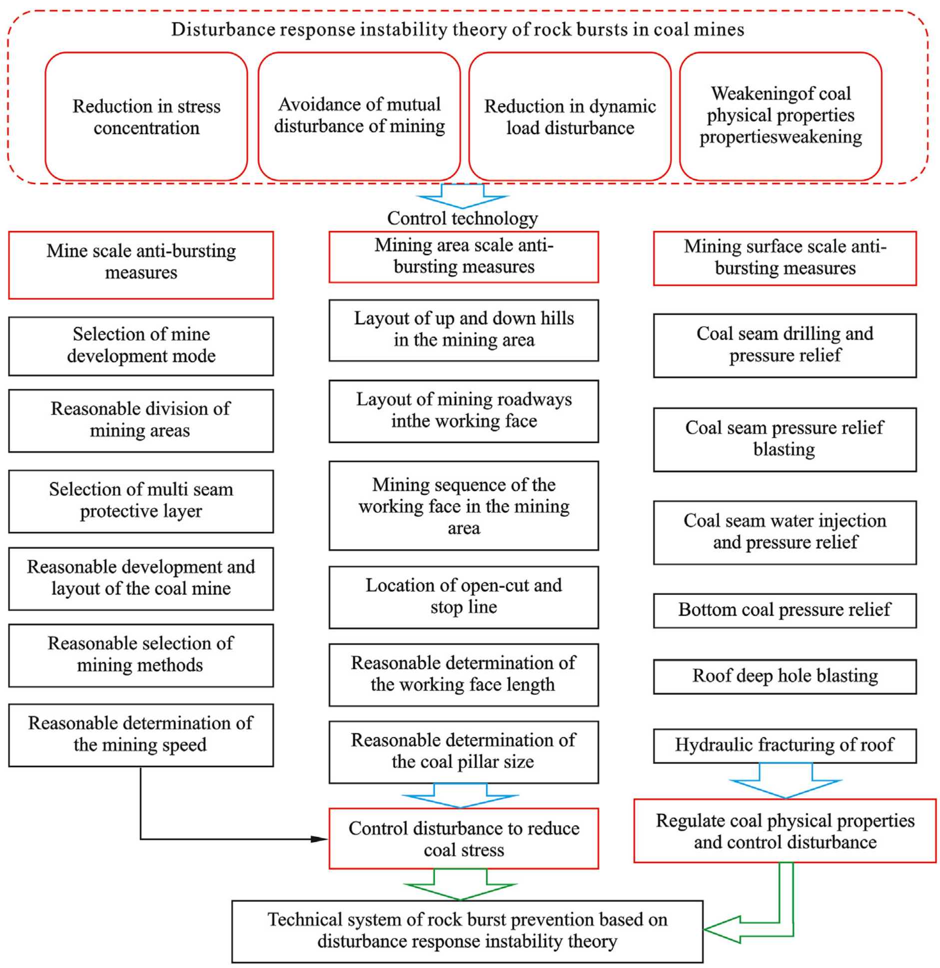

Fig. 16. Technical system of rock burst prevention based on the disturbance response instability theory.

The consumed energy W_s by the plastic zone per unit area of the roadway wall can be obtained by subtitauting the radius of the resistance zone of the rock burst into Eq. (52):

$$W_s = \frac{\sqrt{3}a\sigma_c^2}{16EK} \tag{64}$$

In China, the drilling cutting method and the borehole observation method are commonly used to monitor the radius of the plastic zone in the surrounding rock of a roadway. The absorbed energy is calculated and monitored according to the size of the softening zone.

6. Prevention and control of rock burst based on the disturbance response instability theory

6.1. Technical system for prevention and control of rock bursts

According to the critical stress and critical energy conditions of rock bursts, the disturbance variables should be controlled for the prevention and control of rock bursts. For example, proper development method and protection layer mining can reduce the coal mass stress. In the mining face, reducing dynamic disturbance method, such as roof weakening and fault weakening, should be considered. It can reduce the energy released by the surrounding rock and weaken the dynamic load disturbance. At the same time, the control variables can also be controlled, that is, the physical properties of the coal mass can be altered. For example, coal seam water injection, coal seam drilling, and coal mass blasting can change the bursting liability of the coal mass, increase the energy absorbed by the surrounding rock, and eventually prevent rock bursts. The rock burst prevention and control technology system based on the disturbance response instability theory is shown in Fig. 16.

6.2. Stress-based control

6.2.1. Aiming at disturtance varibles to reduce stress concentration

The main cause of a rock burst is stress concentration in the coal rock mass. In the regional prevention and control of rock bursts, the reduction in stress concentration should be considered firstly. The development and mining methods should be determined reasonably via establishing mining protection layer and proper designing of the mining sequence. In addition, it is required to determine the appropriate length of the working face and avoid overlapped stop line. Widths of the coal pillars in the main roadway, mining area and working face should also be selected reasonably. Furthermore, the mining-induced stress is generated near the excavation, if the mining-induced stresses caused by different mining faces and heading faces are superimposed, the rock burst hazard level increases significantly. A reasonable mining sequence should be determined in the mining arrangement to avoid the influence caused by centralized mining plan.

Fault dislocation may occur in mining process, which will release a large amount of energy and form a fault-dislocation rock burst. Increasing of the mining speed, the bending elastic energy of the roof increases with the increase of exposed length of the cantilever roof. When the roof beam reaches the collapse limit, it suddenly breaks and releases a large amount of elastic energy, inducing the roof fracture type rock burst. Especially for hard roof, the frequency and intensity of the roof fracture type rock burst increase greatly with the increase of mining speed. Therefore, in the regional prevention and control of rock bursts, the mining areas should be divided according to the boundary of large faults. The fault protection coal pillar should be reasonably determined. In this way, the rock burst induced by the fault activation can be avoided.

6.2.2. Aiming at control variables to weaken the physical properties of coal and increase the critical value

The bursting energy index and compressive strength of coal are the control variables of the coal rock deformation system, which determine the critical load of instability. With the decrease in uniaxial compressive strength, the softening area around the roadway increases. It is the resistance area when the rock burst occurs. With the decreasing of the bursting energy index, the rock burst critical load increases. Therefore, in local prevention and control measures, such as drilling, water injection, or blasting of the coal seam, should be undertaken to weaken the coal body and reduce the coal uniaxial compressive strength and bursting energy index.

Coal seam drilling can weaken the coal mechanical properties. With the increase of the borehole number, uniaxial compressive strength σ_c and bursting energy index K gradually decrease [32], as shown in Fig. 17. Through large-diameter drilling, the surrounding rock in a certain distance of the roadway is damaged, forming a weakening zone. As a result, the high stress in the surrounding rock of the roadway is transferred to the deep part of coal mass, reducing the stress in shallow section. After the rock burst is started, the coal body in the weakening zone can absorb the bursting energy, prevent strong vibration of surrounding rock and reduce the ejection of coal body caused by the bursting released energy.

Eq. (35) gives the relationship between the bursting energy index K of coal and the rock burst critical load P_{cr}. It can be observed that as the bursting energy index K increases, the rock burst critical load decreases, rock burst is more likely to occur, and vice versa. It is assumed that a borehole with a radius of d_0 is drilled in the coal seam and the borehole length is L_0. Due to stress concentration, within the radius of $\rho_c = d_0\sqrt{1+\frac{1}{K}}$ around the borehole, damage is caused as the stress exceeds the compressive strength of the coal, which is equivalent to the damage of coal within the original range of $\rho_c L_0$. If boreholes are arranged at a spacing of approximately ρ_c, the failure area of boreholes connects to each other, thus reducing the bursting energy index K of the coal seam. According to the above equation, the rock burst critical load increases, which prevents the rock burst.

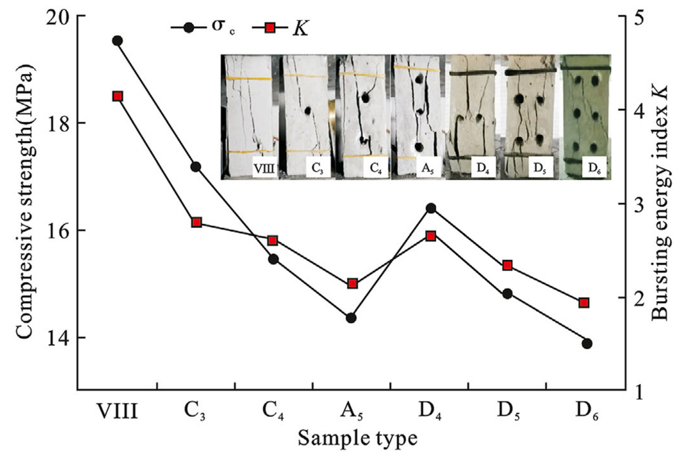

Fig. 17. Mean value of coal seam bursting energy index and drilling density.

Coal seam water injection can prevent and control rock bursts by changing the physical and mechanical properties and bursting liability of coal. With the increase of water content, the compressive strength, cohesion coefficient, internal friction angle, and elastic modulus of coal decrease significantly, and the residual deformation and plasticity index increase. The strain of the coal mass after water injection is much great than that before water injection, and the energy absorption capacity of the coal mass increases when the rock burst occurs. The water content also has a certain impact on the bursting energy index. As the water content increases, the bursting energy index decreases. When the coal seam is saturated, its compressive strength is far lower than that in natural state, which is conducive to the prevention of rock bursts. Table 5 presents the bursting liability test results of coal samples with different water contents from the Gengcun coal mine. It was found that the compressive strength, elastic modulus and bursting energy index of the coal samples are significantly reduced after immersion in water for 3 h and saturation. In addition, the bursting energy index K of the coal samples decreases linearly with the increase in water content ω.

Fig. 18 shows the electromagnetic radiation intensity before and after high-pressure water injection in the 55002 working face of Hutai Coal mine. Before high-pressure water injection, the electromagnetic radiation intensity fluctuated continuously and significantly, with an intensity range of 100–200 mV and an oscillation amplitude of 100 mV. After high-pressure water injection, the electromagnetic radiation intensity basically fluctuated around 100 mV, and the oscillation amplitude was 50 mV. The change in electromagnetic radiation intensity before and after water injection shows that the rock burst hazard level decreases obviously after high-pressure water injection.

Coal seam blasting generates a large number of cracks in the coal body. After blasting, the shock wave first damages the coal body, and then the explosive gas further ruptures the coal body. Due to the air pressure, tangential tensile stress increases around the borehole, resulting in radial tensile fracture. When the stress intensity factor at the front of the fracture is less than the fracture toughness, the fracture is stopped. One point to change of physical and mechanical properties of coal seams are radial fractures, which lead to the decrease of elastic modulus, bursting energy index and uniaxial compressive strength.

Table 5
Parameters of coal sample at different water contents.

Sample No.	Treatment	Moisture content ω (%)	Elastic modulus E (MPa)	Bursting energy index K	Compressive strength (MPa)	Bursting liability
c1	Natural	7.34	0.640	4.238	9.54	Weak
c2	Natural	7.45	0.728	4.347	13.47	Weak
c4	Natural	7.71	0.605	4.223	8.39	Weak
b2	Immersion for 3 h	7.79	0.258	3.615	6.99	Weak
b3	Immersion for 3 h	8.06	0.164	2.473	6.49	Weak
b6	Immersion for 3 h	9.61	0.574	4.105	8.75	Weak
a3	Saturated	8.54	0.802	1.513	8.83	No
a4	Saturated	8.01	0.302	1.444	5.76	No
a6	Saturated	9.28	0.256	1.043	5.39	No

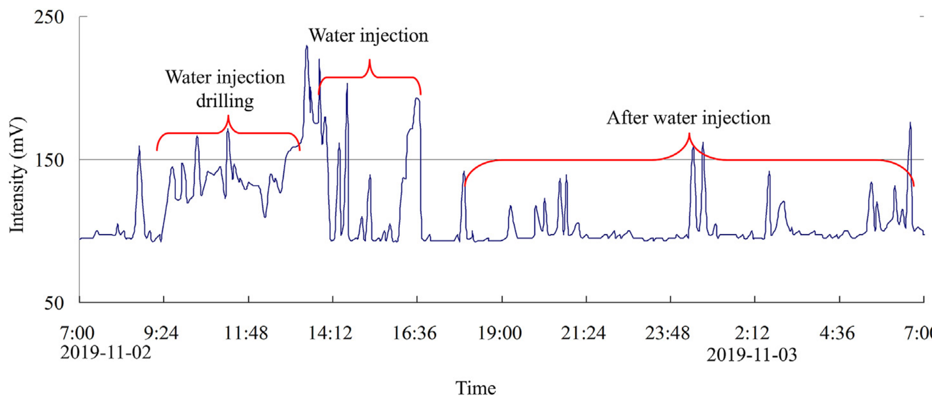

Fig. 18. Electromagnetic radiation intensity before and after high-pressure water injection.

6.2.3. Aiming at support to improve the critical value of rock burst

The condition for rock bursts is that the actual stress of the roadway reaches the critical stress for rock burst. According to Eq. (35), regional anti-bursting measures such as mining consequence and pillar size can be changed to avoid high stress concentration, that is, $P < P_{cr}$. Morevore, measures such as coal seam water injection, pressure relief by drilling, coal seam blasting, and rock bolting can be used to change the coal rock properties and reduce its bursting liability of K. At the same time, the support enhancement increases the roadway support stress p_s and rock burst critical stress P_{cr} for rock burst prevention.

According to the disturbance response instability theory of rock burst, the critical stress of roadway rockburst can be calculated by Eq. (35). Based on the theoretical equation of rock burst critical stress, the anti-bursting safety factor of the roadway support under the specific in-situ stress P is defined as follows:

$$N_s = \frac{P_{cr}}{P} \tag{65}$$

6.3. Energy-based prevention

6.3.1. Reduction of far-field energy release

Equation (53) is the theoretical calculation of the released energy in far-field roof. It can be found that the energy released from the far-field roof is related to the load and self-weight of the overburden of the roof, span of the goaf, thickness of the roof, elastic modulus of the rock, and distance between the roof and the coal seam. The load and self-weight of the overburden of the roof, thickness of the roof, and distance between the roof and the coal seam are often constant, whereas the span of the goaf and elastic modulus of the rock can be modified. Therefore, the roof can be weakened in advance. The elastic modulus and tensile strength of the roof rock can be reduced, so as to reduce the span of the goaf and the energy released from the roof fracture. At present, common roof weakening methods include roof blasting, roof hydraulic fracturing and roof water injection.

Eq. (54) is the theoretical calculation of energy released by the far-field fault dislocation. The energy released by the fault is related to the effective length of the fault strike, rock shear modulus of the fault zone, far-field shear displacement before and after the fault slip, and width of the surrounding rock of the fault. Similarly, fault weakening measures such as fault blasting and water injection can be undertaken to reduce the released energy of the fault. It is also possible to control the displacement caused by fault dislocation and reduce the released energy by fault protection coal pillars.

6.3.2. Increase of energy absorption by surrounding rock

Eq. (52) gives the released energy W per unit length of the roadway in the critical state, and $W = \frac{(1+\mu)\pi a^2 \sigma_c^2}{16E}\left(\frac{1}{K}+1\right)\left(\frac{1}{K}+2\right)^2$. It can be observed that the energy released by the coal mass per unit length in the roadway is related to the roadway radius. From the energy perspective, the bursting damage of the roadway is also an energy absorption process. On this basis, the coal seam boreholes drilled in the surrounding rock of the roadway can be regarded as small-sized "roadways." The calculation method of the energy released during the bursting failure of the borehole follows the same principle as that of the roadway, but the radius is reduced. Therefore, the process of borehole bursting failure is also the process of energy absorption by the surrounding rock. Therefore, by drilling boreholes in the surrounding rock of the roadway, the energy consumption of borehole bursting damage can be controlled. In addition, the damping energy consumption of coal can also be increased by coal seam water injection and coal blasting.

6.3.3. Increase of energy absorbed by support

The elastic energy should be dissipated by the support as much as possible to reduce the residual bursting energy that damages the roadway [33]. An anti-bursting support design from both energy and stress should be considered. When considering the energy absorption by the support, following processes are mainly involved, as shown in Fig. 19:

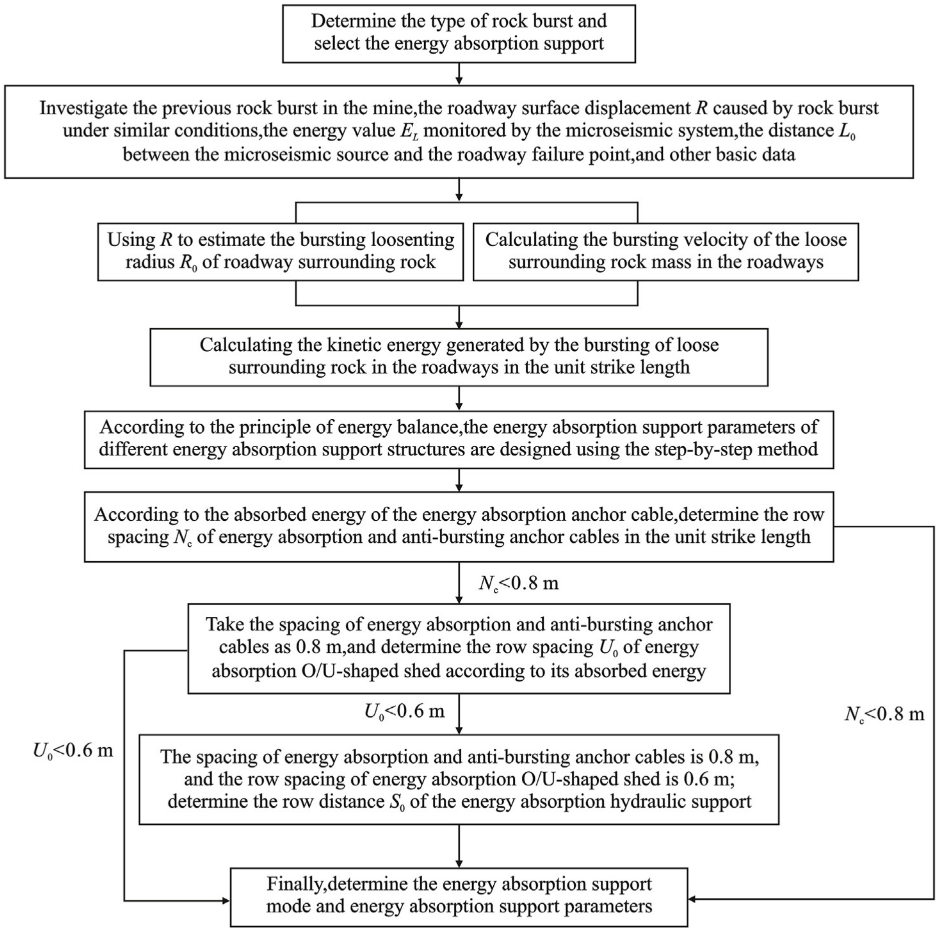

Fig. 19. Flowchart of the energy calculation for energy absorption of support [34].

(1) Investigation of roadway damage caused by rock burst
(2) Estimation of the loose circle radius of the roadway
(3) Calculation of rock mass bursting velocity in the loose range of the roadway
(4) Calculation of the kinetic energy generated by surrounding rock bursting
(5) Determined that the kinetic energy generated by loose rock mass that is just absorbed by the energy absorbing supporting structure in unit length. From the front, each anchor bolt can absorb energy of 30 kJ, each anchor cable can absorb energy of 70 kJ, each hydraulic support can absorb energy of 479.6 kJ.

For the same type of rock bursts with different among released energy, the anchor support parameters are first selected according to the relevant standards, and the support spacing N_c of the energy absorption and anti-bursting anchor cables in the unit length is calculated. If $N_c < 0.8$ m, the 2nd level energy absorption support is adopted, N_c is taken as 0.8 m. The parameters of the U-steel support in the roadway are calculated, and the row spacing U_0 of the retractable support (U-shaped steel support) in the roadway is determined. If U_0 is less than 0.6 m, the 3rd level energy absorption support is adopted, N_c is taken as 0.8 m and the row spacing U_0 of the U-shaped steel support in the roadway is 0.6 m. The parameters of the energy absorption hydraulic support are calculated and its row spacing is determined.

The three-level energy absorption support composed of the energy absorption anchor cables and O-shaped shed. Anti-bursting hydraulic support is adopted within 200 m ahead of the two mining roadways of the 513 working face in Longjiapu coal mine, as shown in Fig. 20. The

Fig. 20. Application of anti-bursting support in the roadway.

anchor net, energy absorption anchor cable, 36U-6.0 m O type shed support, hydraulic lifting shed, and ZHDF4150/52/36 type anti-bursting hydraulic support are used for the three-level support. In 2021, there were two microseismic events with energy greater than 3E+07 J in 513 working face. The roadway maintained its good condition, and there were no casualties.

7. Conclusions

(1) In this study, the disturbance response instability theory of rock bursts in coal mines is presented, and the critical stress and capacity conditions of rock bursts are determined. The stability of the coal rock mass deformation system in a roadway is controlled by the coal uniaxial compressive strength, bursting energy index, roadway radius, and support stress. The rock bursts can be considered as the instability of the coal rock mass deformation system under control, disturbance, and response variables.

(2) Based on the disturbance response instability theory of rock bursts in coal mines, the critical stress index method for rock burst hazard assessment is established by comparing the measured in-situ stress P with the critical stress P_{cr}.

(3) It is proposed that the rock burst hazard can be tracked by monitoring the coal stress and the bursting released energy and comparing them with the critical stress and energy of rock bursts. In addition, a monitoring and early warning system is established and engineering practice is carried out.

(4) From the two aspects of stress control and energy control, the prevention and control methods of rock bursts are presented. The prevention and control mechanism of rock bursts is revealed, the prevention and control technology system is established, and the engineering application is carried out.

Funding

This study was financially supported by the National Natural Science Foundation of China (51974150 and U1908222) and National key research and development program (2022YFC3004605).

Declaration of competing interest

The authors declare that they have no known competing financial interests or personal relationships that could have appeared to influence the work reported in this paper.

Acknowledgements

The authors gratefully acknowledge the support from some staff of Institute of Geohazard Mechanics in Liaoning University and the Research Institute of Rock burst (RIRB) of Liaoning province. We would like to thank Editage (www.editage.cn) for English language editing.

References

[1] Yishan Pan, Coal Mine Rock Burst, Science Press, Beijing, 2018.
[2] Mahdi Askaripour, Saeidi Ali, Alain Rouleau, et al., Rockburst in underground excavations: a review of mechanism, classification, and prediction methods, Undergr. Space 7 (4) (2022) 577–607.
[3] N.G.W. Cook, E. Hoek, J.P.G. Pretorius, et al., Rock mechanics applied to the study of rockbursts, South Afr. Inst. Min. Metall. 66 (10) (1965) 435–528.
[4] Z.T. Bieniawski, H.G. Denkhaus, U.W. Vogler, Failure of fractured rock, Int. J. Rock Mech. Min. Sci. Geomech. Abstr. 6 (3) (1969) 323–330.
[5] I.M. Petukhov, A.M. Linkov, The theory of post-failure deformations and the problem of stability in rock mechanics, Int. J. Rock Mech. Min. Sci. Geomech. Abstr. 16 (1979) 57–76.
[6] Yusheng Li, Wanbin Zhang, Shukun Wang, Study of rockburst mechanism, China Coal Soc. 9 (4) (1984) 81–83.
[7] Mentao Zhang, Study of rockburst mechanism, Fuxin Min. Inst. (s1) (1985) 65–72.
[8] Mengtao Zhang, Zenghe Xu, Yishan Pan, et al., Unified instability theory of rockburst and outburst, China Coal Soc. 16 (4) (1991) 48–53.
[9] Yishan Pan, Xuebin Wang, Zhonghua Li, Analysis of the strain softening size effect for rock specimens based on shear strain gradient plasticity theory, Int. J. Rock Mech. Min. Sci. 39 (2002) 801–805.
[10] Yishan Pan, Zhonghua Li, Analysis of rock structure stability in coal mines, Int. J. Numer. Anal. Methods Geomech. 29 (2005) 1045–1063.
[11] Qingxin Qi, Yishan Pan, Haitao Li, et al., Theoretical basis and key technology of prevention and control of coal-rock dynamic disasters in deep coal mining, China Coal Soc. 45 (5) (2020) 1567–1584.
[12] Linming Dou, He Jiang, Anye Cao, et al., Rock burst prevention methods based on theory of dynamic and static combined load induced in coal mine, China Coal Soc. 40 (7) (2015) 1469–1476.
[13] Fuxing Jiang, Wang Ping, Zengqiang Feng, et al., Mechanism, prediction and control of "rock burst induced by shock bump" kind dynamic accident in composite thickness coal, China Coal Soc. 34 (12) (2009) 1605–1609.
[14] Junfeng Pan, Yu Ning, Debing Mao, et al., Theory of rockburst start-up during coal mining, Chin. J. Rock Mech. Eng. 31 (3) (2012) 586–596.
[15] A. Manouchehrian, M. Cai, Numerical modeling of rockburst near fault zones in deep tunnels, Tunn. Undergr. Space Technol. 80 (2018) 164–180.
[16] A. Manouchehrian, M. Cai, Influence of material heterogeneity on failure intensity in unstable rock Failure, Comput. Geotech. 71 (2016) 237–246.
[17] Onur Vardar, Chengguo Zhang, Ismet Canbulat, et al., A semi-quantitative coal burst risk classification system, Int. J. Min. Sci. Technol. 28 (5) (2018) 721–727.
[18] Hadi Farhadian, A new empirical chart for rockburst analysis in tunnelling: tunnel rockburst classification (TRC), Int. J. Min. Sci. Technol. 31 (4) (2021) 603–610.
[19] Łukasz Wojtecki, Sebastian Iwaszenko, Derek B. Apel, et al., Use of machine learning algorithms to assess the state of rockburst hazard in underground coal mine openings, Rock Mech. Geotech. Eng. 14 (3) (2022) 703–713.
[20] Petr Konicek, Mani Ram Saharan, Hani Mitri, Destress blasting in coal mining-state-of-the-art review, Procedia Eng. 26 (2011) 179–194.
[21] Krzysztof Fuławka, Piotr Mertuszka, Witold Pytel, Seismic evaluation of the destress blasting efficiency, Rock Mech. Geotech. Eng. 14 (5) (2022) 1501–1513.
[22] Charlie Chunlin Li, Mikula Peter, Brad Simser, et al., Discussions on rockburst and dynamic ground support in deep mines, Rock Mech. Geotech. Eng. 11 (2019) 1110–1118.
[23] Charlie Chunlin Li, Principles and methods of rock support for rockburst control, Rock Mech. Geotech. Eng. 13 (1) (2021) 46–59.
[24] Yaodong Jiang, Yishan Pan, Fuxing Jiang, et al., State of the art review on mechanism and prevention of rock bursts in China, China Coal Soc. 39 (2) (2014) 205–213.
[25] Zhonghua Li, Yishan Pan, Forecast on the magnitude of rock burst in circle chamber, Coal Min. Technol. (3) (2003) 4–6.
[26] Yishan Pan, Lianpeng Dai, Theoretical formula of rock burst in coal mines, China Coal Soc. 46 (3) (2021) 789–799.
[27] Yishan Pan, Disturbance response instability theory of rockburst in coal mine, China Coal Soc. 43 (8) (2018) 2091–2098.
[28] Tianwei Shi, Yishan Pan, Aiwen Wang, et al., Classification of rock burst in coal mine based on energy storage and release bodies, China Coal Soc. 45 (2) (2020) 524–532.
[29] Aiwen Wang, Gang Wang, Lianpeng Dai, et al., Evaluation on the rock burst risks of tunnel using critical stress index method, China Coal Soc. 45 (5) (2020) 1626–1634.
[30] Llianpeng Dai, Yishan Pan, Z.H. Li, et al., Quantitative mechanism of tunnel rockbursts in deep extra-thick coal seams: theory and case histories, Tunn. Undergr. Space Technol. 111 (2021) 1–14.
[31] A. Mcgarr, Seismic moments and volume change, Geophys. Res. 81 (8) (1976) 1487–1494.
[32] Aiwen Wang, Qianshu Gao, Yishan Pan, et al., Bursting liability and energy dissipation laws of prefabricated borehole coal samples, China Coal Soc. 46 (3) (2021) 959–972.
[33] Chunchen Wei, Chengguo Zhang, Ismet Canbulat, et al., Evaluation of current coal burst control techniques and development of a coal burst management framework, Tunn. Undergr. Space Technol. 81 (2018) 129–143.
[34] Aiwen Wang, Dewei Fan, Yishan Pan, et al., Determination of three-level energy absorbing support parameters in rock burst tunnel based on energy calculation, Coal Sci. Technol. 49 (6) (2021) 72–81.